JOURNAL OF MATERIALS SCIENCE **36** (2001) 4661–4671

A fractal Cantor set based description of interlaminar contact evolution during thermoplastic composites processing

F. YANG, R. PITCHUMANI*
Composites Processing Laboratory, Department of Mechanical Engineering, University of Connecticut, Storrs,Connecticut 06269-3139, USA
E-mail: pitchu@engr.uconn.edu

Fusion bonding is the principal phenomenon governing the fabrication of layered thermoplastic-matrix composites using techniques such as tow placement and tape laying. An important step in fusion bonding is the *intimate contact* process, which refers to the development of interfacial contact area between thermoplastic plies, caused by the spreading of the surface asperities. The contacted areas, in turn, form sites for molecular interdiffusion which leads to interfacial bonding. The geometric complexity of the surface asperity profiles presents a fundamental challenge to an effective description of the intimate contact process. Toward addressing the challenge, this paper presents a model for interfacial contact area development utilizing the fractal properties of thermoplastic ply surfaces. Using a Cantor set representation of the surfaces, and a squeeze flow model to describe their spreading during the processing, the interfacial contact area evolution is related to the process parameters and the geometric parameters in the fractal surface description. The model predictions are shown to compare well with experimental data for several thermoplastic materials.

Nomenclature

a	height of a generic rectangular asperity at time t [m]
$a_{n,0}$	initial height of (n)th generation asperity [m]
$a_{n,f}$	final height of (n)th generation asperity [m]
b	width of a generic rectangular asperity at time t [m]
$b_{n,0}$	initial width of (n)th generation asperity [m]
$b_{n,f}$	final width of (n)th generation asperity [m]
D	fractal dimension of rough surfaces
D_{ic}	degree of intimate contact
f	scaling ratio between two adjacent generations of asperities in the Cantor set
$\hat{F}$	force applied to an asperity of unit depth [N/m]
h_0	recess depth of the first generation asperities [m]
h_n	recess depth of the $(n-1)$th generation asperities [m]
L_0	total horizontal length of the Cantor set block [m]
L_n	total horizontal length of the (n)th generation asperities [m]
L_i	linear contact area of the fractal surface with a plane [m]
p	pressure inside a generic asperity at location ξ and time t [N/m^2]
p_0	ambient pressure [N/m^2]
p_{app}	applied consolidation pressure [N/m^2]
s	number of asperities on a repeating segment of the Cantor set block
$S(\omega)$	power spectrum [m^3]
t	time [s]
u	displacement of the contact plane from its initial position [m]
u_n	cumulative displacement of the flattening of asperities of generation $\geq n$ [m]
v_ξ	average velocity of the squeeze flow inside an asperity [m/s]

Greek symbols

μ	viscosity of the thermoplastic material [Ns/m^2]
σ	standard deviation of rough surface profile [m]
ω	frequency on the power spectrum [m^{-1}]
ξ	coordinate along the interface [m]

1. Introduction

Fabrication of layered thermoplastics and thermoplastic-matrix composites using processes such as tow placement, tape laying, resistance welding, and autoclave forming is fundamentally based on the principle of fusion boding, which involves applying heat and pressure to two contacting thermoplastic surfaces. The applied

*Author to whom all correspondence should be addressed.

temperature and pressure cause the interfacial contact area to increase by the spreading of the softened surface asperities—a process referred to as *intimate contact*—while the elevated temperatures initiate intermolecular diffusion processes, termed autohesion, across the areas in intimate contact. The intimate contact process, therefore, forms a prerequisite for the development of interlaminar bond strength in the composite.

The intimate contact development is strongly influenced by the processing parameters—pressure, temperature, and time—and the surface geometric parameters. A reliable description of the interfacial contact evolution as a function of the governing parameters is essential for arriving at effective process designs in practice. Modeling of the intimate contact process fundamentally requires a description that captures the intrinsic features of the asperity structures on thermoplastic ply surfaces. The geometric complexity of the surface asperities, however, have posed a challenge to their quantitative description, and in turn, of the intimate contact process.

A model for intimate contact was presented by Dara and Loos [1], in which the thermoplastic surface asperity profiles were treated as a distribution of rectangular elements of different sizes. Lee and Springer [2] followed this model with a simplification of the geometry, taking the idealized rectangular elements to be of the same size. Although these models have been used to describe the processing of specific material systems, a principal limitation lies in the fact that the geometric parameters of the rectangular elements can not be determined directly from the surface profilometric measurements; the parameters are used as tuning factors to fit the model to experimental data. Besides, the model geometries considered do not reflect the intrinsic multiscale characteristics of real surfaces, such as that shown in Fig. 1a, which is a profilometric scan of an AS4/PEEK tow (from Cytec Fiberite, Inc.). The objective of the present study is to overcome the aforementioned drawbacks.

A fundamental view of thermoplastic surfaces (Fig. 1a) reveals that the geometric structure is random, and that the roughness features are found at a large number of length scales. Further, Fig. 1b shows that the power spectrum of the asperity profile, obtained as a Fast Fourier Transform (FFT) of the profilometric scan in Fig. 1a, exhibits a power-law variation with the spatial frequency (equivalently, the asperity scale). This suggests the existence of a fractal structure formed by the asperity elements in the profile, implying that when a portion of the asperity surface is magnified appropriately, the magnified structure will be statistically similar to the original [3–7]. A fractal geometry based description, which accounts for the roughness features at multiple length scales, may therefore be more appropriate for describing the surface asperities and their spreading process. This forms the basis of the model developed in this article.

A fractal Cantor set construction is used to represent the multiscale asperity structures on thermoplastic ply surfaces. A squeeze flow model based on the fractal description is then developed to simulate the intimate contact evolution as a function of the process and surface parameters. It is shown that the parameters of the Cantor set can be obtained directly from the surface profilometric scans. Parametric studies are presented to illustrate the effects of the geometric parameters on the contact area development. The model is validated using experimental data on different thermoplastic materials, over a wide range of processing parameters.

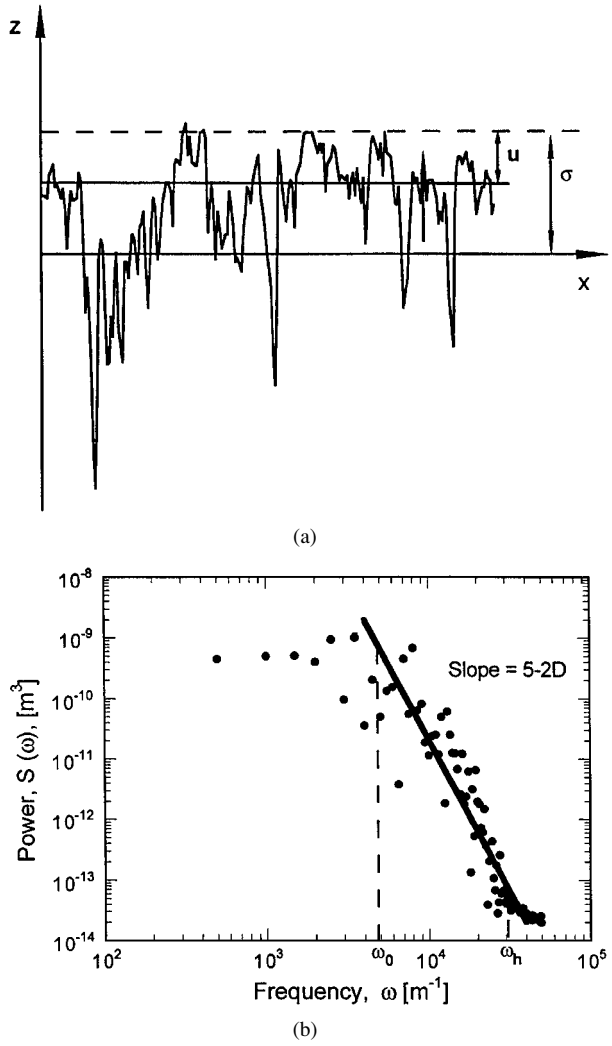

Figure 1 (a) Surface profile scan of AS4/PEEK tow and (b) its power spectrum.

2. Cantor set description of rough surfaces

As seen in Fig. 1, measurements of thermoplastic surface profiles show that their asperity sizes cover several length scales. Intimate contact development depends on the spreading of all of these asperities. As pointed out by Mandelbrot [3], most rough surfaces have a statistically self-affine structure, which means that a small portion of a surface will be the same as a large portion if it is magnified appropriately in different coordinate directions. The contact between two rough surfaces can be modeled as contact between an equivalent rough surface and a rigid flat surface [6]. Following Borodich and Mosolov [5] and Warren *et al*. [6], the self-affine characteristic of a rough surface is described by a Cantor set model in this paper.

The construction of a Cantor set surface, shown in Fig. 2a, is as follows: Starting from a rectangle of length L_0 and an arbitrary height, a small rectangle of height

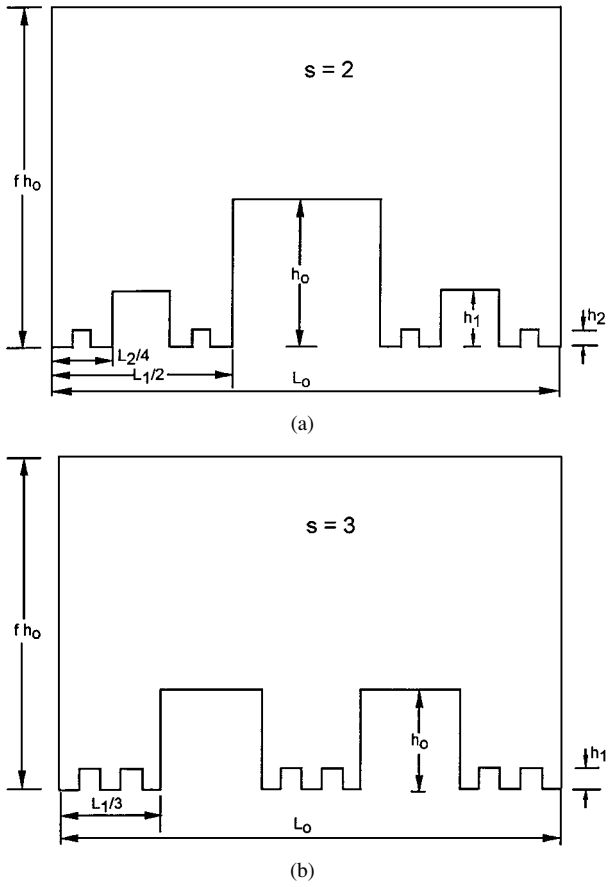

Figure 2 Cantor set fractal surfaces with (a) $s = 2$ and (b) $s = 3$.

h_0 is removed from the middle, so that the remaining length of the rectangle is $L_1 = L_0/f$, where the scaling factor $f > 1$. This results in two identical rectangles of height h_0 and width $L_1/2$, which are called the first generation asperities. Next, from each of the first generation asperities, a rectangle of height $h_1 = h_0/f$ is removed, which yields four rectangular asperity elements of height h_1 and width $L_2/4$, where $L_2 = L_1/f$. Continuing the procedure results in the self-affine Cantor set in Fig. 2a. Note that in the above procedure, one rectangle is removed from each asperity which results in $s = 2$ smaller asperities. In the case shown in Fig. 2b, two rectangles are removed from each asperity, resulting in $s = 3$ of the next generation asperities. The total horizontal length and recess depth of the (n)th generation asperities are given by,

$$L_n = \left(\frac{1}{f}\right)^n L_0; \qquad h_{n-1} = \left(\frac{1}{f}\right)^{n-1} h_0 \tag{1}$$

In the above development, an equal scaling has been employed in describing the lengths and widths of the asperity elements in the Cantor set block. A more general description based on nonidentical scaling f_x and f_z along the length and height of the Cantor set, respectively, has been reported by Warren *et al.* [6], i.e., $L_n = (\frac{1}{f_x})^n L_0$ and $h_{n-1} = (\frac{1}{f_z})^{n-1} h_0$. A single scaling factor, $f = f_x = f_z$, was used in the present study for model simplicity, and was supported by the observation that the measured f_x and f_z values were nearly identical for actual thermoplastic tow surface profiles, as demonstrated later in this section.

Starting from the self-affine scaling of a rough surface and statistical considerations, the fractal dimension of the Cantor set surface, D, may be related to the scaling factor, f, and s. Such a relationship was derived by Warren *et al.* [6] for the general case of nonuniform scaling using distinct scaling factors, f_x and f_z, as

$$D = 1 - \frac{\ln f_z}{\ln s f_x} + \frac{\ln s}{\ln s f_x}$$

For the case of equal scaling, considered in this paper, the foregoing relationship may be simplified by setting $f_x = f_z = f$, to obtain $D = 2 \ln s / \ln sf$ or equivalently,

$$s = f^{\frac{D}{2-D}} \tag{2}$$

The fractal parameters D, L_0, h_0, f, and s in the above description can be determined from the roughness measurements as discussed below.

- For a given thermoplastic tape, its surface profile, $z(x)$, may be obtained using a contact or noncontact profilometer. Using Fourier's theorem the surface profile function, $z(x)$, can be spectrally decomposed into its components of sine and cosine waves, whose amplitudes can be determined from the profile's power spectrum obtained using a fast Fourier transformation. It can be shown that for a fractal surface, its power spectrum $S(\omega)$ follows a power law of the form [3]

$$S(\omega) = \frac{C}{\omega^{5-2D}} \tag{3}$$

  where C is a constant, and ω is the frequency (or the wave number), which denotes the reciprocal of the length scale. The power law suggests the self-affine scaling of a fractal surface mentioned above, where the parameter D is the fractal dimension of the profile. As mentioned by Borodich and Mosolov [5] and Majumdar and Bhushan [7], the power law variation is observed within a finite interval of frequencies (ω_0, ω_h). The surface profile measurements of AS4/PEEK and IM-7/PIXA-M thermoplastic tapes also reveal the existence of a distinct interval in which the power spectrum obeys a power law; outside of this interval, the power spectrum deviates from the power law, as seen Fig. 1b. The fractal dimension, D, can be determined from the slope of a log-log plot of the power spectrum with respect to the frequency, ω, within the frequency range $\omega_0 \leq \omega \leq \omega_h$.
- The upper limit of the frequency interval, ω_h, corresponds to the smallest length scale in the surface profile while the lower limit, ω_0, is associated with the largest repeating unit in the profile. Hence, the lower bound ω_0 of the interval is chosen in this study to determine the length L_0 of the Cantor set block, as $L_0 = \frac{1}{\omega_0}$.
- Since h_0 denotes the largest asperity height in the Cantor set model, its value may be estimated based on the standard deviation, σ, of the surface roughness profile. Considering the asperity features within a $\pm\sigma$ range about the mean to be dominant in the intimate contact process, h_0, is evaluated as 2σ.

- For the contact process between a Cantor set surface and a flat surface, the linear contact area of the fractal surface with the plane, L_i, is related to the displacement, u, of the plane by following an approach similar to that in ref. [6], but using $f_x = f_z = f$. The resulting expression is given by

$$L_i = \frac{\sigma - u}{f(h_0/L_0)} \tag{4}$$

  From a real surface profile, L_i may be evaluated as the total intercepted lengths of the profile with horizontal lines at various displacement, $\sigma - u$, from the profile mean (see Fig. 1). The parameter f can then be obtained by a statistical regression of the measured intercepted length data over the range $0 \leq u \leq 2\sigma$ to Equation 4. In order to verify the appropriateness of using a single scaling factor, f, the measurements on actual thermoplastic surface profiles were fitted to the linear contact area expression using the two scaling factors, f_x and f_z, given by Equation 29 of ref. [6]. It was found that for all the thermoplastic materials used in the study, f_x and f_z values were close to each other. For example, in the case of AS4/PEEK, $f_x = 1.351$ and $f_z = 1.354$. Therefore, as mentioned above, only one scaling factor, f, was used in this paper to reduce the number of parameters in the model.
- The parameter s can be determined using the measured values of f and D in Equation 2.

Note that in the above description, all the fractal parameters are uniquely determined for a surface from its profile measurements. In the next section, the fractal description is used to model the interfacial contact area evolution during the intimate contact process.

3. Intimate contact process model

Based on the thermoplastic surface description developed in the preceding section, the intimate contact process can be modeled as the flattening of the Cantor set surface by a rigid half plane, as shown in Fig. 3a. When the asperities from the $(n+1)$th generation are deformed, the (n)th and lower generations are supposed to retain their shape and all the deformed material is considered to flow into the troughs between the $(n+1)$th generation asperities. Note that all the asperities in the Cantor set model are rectangles of various sizes, hence we first consider the problem of squeeze flow of a generic rectangle in Fig. 3b. The terms a_0 and b_0 are the initial height and width of the rectangle, respectively, and a and b are the height and width at time t.

The squeeze flow is assumed to be one-dimensional in the direction transverse to the fiber. This is justified by the fact that the viscosity in the direction parallel to the fibers is much larger than that in the transverse direction. Applying the principle of conservation of mass to a differential segment $d\xi$ in Fig. 3b yields,

$$a\frac{dv_\xi}{d\xi} + \frac{da}{dt} = 0 \tag{5}$$

where ξ is the coordinate along the interface. By assuming laminar flow, the average velocity, v_ξ, is given

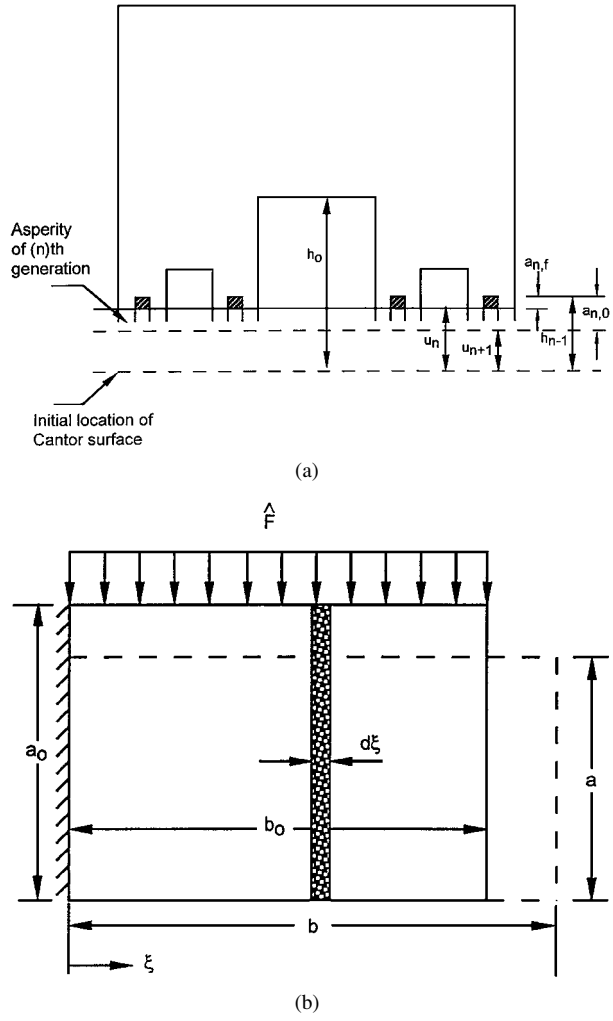

Figure 3 (a) Deformation of a Cantor set surface by a contact plane, and (b) squeeze flow of a generic rectangular asperity element.

by [8, 9]

$$v_\xi = -\frac{a^2}{12\mu}\frac{dp}{d\xi} \tag{6}$$

where μ is the viscosity of the softened asperities, and $\frac{dp}{d\xi}$ is the pressure gradient along the flow direction. Note that a, p and v_ξ are all functions of location ξ and time t. Substituting Equation 6 into Equation 5 yields a second order differential equation for the pressure, which is subject to the following boundary conditions

$$\frac{dp}{d\xi}(\xi = 0, t) = v_\xi(\xi = 0, t) = 0; \quad p(\xi = b, t) = p_0 \tag{7}$$

where p_0 is the ambient pressure.

Solving Equations 5–7, the pressure distribution can be determined as a function of ξ. The force applied per unit depth, $\hat{F}$, to the rectangle may then be obtained as:

$$\hat{F} = \int_0^b (p - p_0)\, d\xi = \int_0^b \frac{6\mu}{a^3}\frac{da}{dt}(\xi^2 - b^2)\, d\xi$$
$$= -4\mu\frac{da}{dt}\frac{b^3}{a^3}$$

Integrating the final expression with respect to time, subject to the initial condition $a(t=0) = a_0$, and

asperity volume conservation $a_0 b_0 = ab$, we get

$$\int_0^t \frac{\hat{F}}{\mu}\, dt = \frac{4(a_0 b_0)^3}{5}\left(\frac{1}{a^5} - \frac{1}{a_0^5}\right) \tag{8}$$

Equation 8 shows that the height, a, of one element is a function of time t, the applied force $\hat{F}$, the viscosity μ of the softened asperity, and the initial geometry $a_0,\ b_0$.

With the foregoing description of the squeeze flow of a rectangular asperity as basis, the degree of intimate contact for a Cantor set may be obtained as a function of time. The degree of intimate contact is defined as the fraction of the interfacial area that is in contact. The contact process starts with the squeeze flow of the highest generation asperities (theoretically, asperities at generation ∞), and progressively goes to the first generation asperities. As mentioned before, when the $(n+1)$th generation asperities are being compressed, the deformed material flows into the troughs between the asperity elements. When the troughs are completely filled, the $(n+1)$th generation asperities are then combined into the (n)th generation, and the process proceeds with the deformation of the (n)th generation asperities. This process goes from $n = \infty$ to $n = 1$ mathematically.

In order to describe this process, we introduce u_n (see Fig. 3a) as the cumulative displacement of the Cantor surface, measured from its initial state, resulting from the flattening of asperities of generations $\geq n$. The cumulative displacement, u_n, can be determined from volume conservation; i.e., using the fact that the total volume of the asperities of generations $\geq n$ will fill the troughs of and combine into the $(n-1)$th generation asperities. In terms of the known parameters of the Cantor set surface, we get the expression

$$u_n = \frac{h_0}{f^{n-2}(f+1)} \tag{9}$$

Note that Equation 9 can also be obtained starting with the following expression for the displacement given by Warren *et al*. [6] in terms of the distinct scaling factors, f_x and f_z

$$u_n = \frac{\left(1 - \frac{1}{f_x}\right)h_0}{f_z^{n-1}} \sum_{k=0}^{\infty} \left(\frac{1}{f_z f_x}\right)^k$$

It is left as an exercise for the reader to verify that Equation 9 results by substituting $f_x = f_z = f$ in the above equation and evaluating the convergent infinite series, followed by simplifying the resulting expression.

Equation 8 is used to determine the degree of intimate contact development as a function of time for the (n)th generation asperities. The input information for Equation 8 is the initial length $b_{n,0}$ and height $a_{n,0}$, and the final height $a_{n,f}$ of the asperities. It follows from the Cantor set construction that the total number of the (n)th generation asperities is $N = s^n$ and that the initial length of each asperity is then $b_{n,0} = L_n/N$. Based on consideration of volume conservation, the initial height of each asperity is $a_{n,0} = h_{n-1} - u_{n+1}$ as indicated in Fig. 3a. The final height $a_{n,f}$ is the asperity height when the (n)th generation fuses with the $(n-1)$th generation, hence, $a_{n,f} = h_{n-1} - u_n$ (Fig. 3a), where h_n and h_{n-1} are given by Equation 1. From its definition, the degree of intimate contact, $D_{ic}^{(n)}(t)$, for the (n)th generation asperities at any time instant, t, can be expressed as

$$D_{ic}^{(n)}(t) = \frac{N b_n}{L_0} = \frac{s^n a_{n,0} b_{n,0}}{L_0 a_n} \tag{10}$$

where a_n and b_n are height and length of the (n)th generation of asperities at time t, and the mass conservation principle, $a_n b_n = a_{n,0} b_{n,0}$, is used to obtain the final expression above. Using Equation 8 and expressing $\hat{F}$ as $L_0 p_{app}/N$, we have

$$\frac{L_0}{N}\int_{t_{n+1}}^{t} \frac{p_{app}}{\mu}\, dt = \frac{4(a_{n,0} b_{n,0})^3}{5}\left(\frac{1}{a_n^5} - \frac{1}{a_{n,0}^5}\right); \quad t_{n+1} \leq t \leq t_n \tag{11}$$

where p_{app} is the applied gage pressure, t_{n+1} is the start time for the consolidation process of the (n)th generation asperities, i.e., $a_n = a_{n,0}$, and t_n is the time when $a_n = a_{n,f}$. Equations 10 and 11 yield

$$D_{ic}^{(n)}(t) = \frac{1}{f^n}\left[\frac{5}{4}\left(\frac{h_0}{L_0}\right)^2 \frac{f^{\frac{2nD}{2-D}+n+4}}{(f+1)^2}\int_{t_{n+1}}^{t} \frac{p_{app}}{\mu}\, dt + 1\right]^{1/5}, \quad t_{n+1} \leq t \leq t_n \tag{12}$$

where $a_{n,0}$ and $b_{n,0}$ have been related to the parameters of the thermoplastic surface, D, f, and h_0/L_0, using Equations 1, 2, and 9. Note that the foregoing equations pertain to the (n)th generation asperities being in contact with the rigid flat plane. The degree of intimate contact evolution at any time t is obtained by recording the process as follows: First, the start time and the end time, t_{n+1} and t_n respectively, for the compression of each generation are calculated using Equation 8. Next, the generation, (n), whose start and end times encompass the desired time t is determined. The degree of intimate contact is then obtained by using Equation 12 for this generation.

4. Experimental investigations

Experimental studies were conducted on thermoplastic prepregs, IM-7/PIXA-M and AS4/PEEK from Cytec Fiberite Inc. with the primary objective of validating the fractal intimate contact model. It is evident from Equation 12 that the evaluation of the model requires information on the fractal parameters, D, f, and h_0/L_0, describing the thermoplastic prepreg surface geometry, and the viscosity, μ, of the prepreg material. The measurement of these parameters is discussed first. Furthermore, systematic experiments on the fusion bonding of the thermoplastic prepreg tapes and tows at isothermal conditions were carried out at different pressures and temperatures. The processing experimental measurement of the degree of intimate contact for the fabricated specimens is also described in this section.

Profile measurements on the thermoplastic prepregs were conducted using a profilometer ALPHA-STEP 2000 from Tencor Instruments. The profilometer has a diamond stylus of radius 2.5 μm and its vertical resolution is 5 Å. The scan lengths ranged from 80 μm

TABLE I Fractal surface geometric parameters for AS4/PEEK and IM-7/PIXA-M materials

Prepreg material	f	D	h_0/L_0
AS4/PEEK	1.45	1.32	0.050
IM-7/PIXA-M	1.40	1.38	0.018

to 10 mm with each scan having 200–2000 evenly spaced data points. For the two materials, AS4/PEEK and IM-7/PIXA-M, the surface profile scans recorded at several locations on the surfaces were analyzed to determine fractal dimension, D, and the Cantor set parameters f and h_0/L_0 using the procedures described in Section 2. An example profile of AS4/PEEK with a scan length of 10 mm is shown in Fig. 1a. It was found that in the spatial frequency (wave number) range 4.8×10^3 m^{-1} to 3.0×10^4 m^{-1}, its power spectrum in Fig. 1b follows a power law which corresponds to a fractal dimension of $D = 1.32$. The geometric parameters measured on the material surfaces are summarized in Table I.

The viscosity data of AS4/PEEK was taken from the literature [8], while the viscosity of IM-7/PIXA-M prepreg was measured in this study following the procedure commonly used for characterizing the rheology of fiber-reinforced thermoplastic material [10]. The measurement is based on the principle of one-dimensional squeeze flow developed in Equation 8, as applied to the compression of prepreg sheets. At constant temperature and pressure, Equation 8 can be transformed to: $\left(\frac{1}{a^5} - \frac{1}{a_0^5}\right) \propto \frac{t}{\mu}$, where a_0 is the initial thickness (height) of the prepreg ply, and a is its thickness at any time t. Plotting the term on the left hand side versus time t, the viscosity is obtained as the inverse of the slope of the resulting linear variation. In the experiments, 1-inch wide IM-7/PIXA-M prepregs were stacked up to an initial height, a_0, of 0.04 inches and placed in a hot press as shown in Fig. 4. The desired pressure and temperature were applied for a period of time, t, and then the sample was removed and its height, a, was measured. This procedure was executed over a range of pressures and temperatures and the measured viscosity results are listed in the Table II, as a function of temperature.

The viscosity of IM-7/PIXA-M, which has an amorphous polyimide matrix, may be represented over the temperature range T_g to $T_g + 100$ by a Williams-Landel-Ferry (WLF) function of the form [10]

$$\mu(T) = \mu(T_g) \exp\left[\frac{-C_1(T - T_g)}{C_2 + (T - T_g)}\right] \qquad (13)$$

where $T_g = 250°$C is the glass transition temperature of the PIXA-M polyimide resin. Fitting the data in Table II to Equation 13, the constants are obtained as $\mu(T_g) = 8.85 \times 10^9$ Pa · s, $C_1 = 13.94$, $C_2 = 9.62$ K.

TABLE II Temperature-dependent viscosity of IM-7/PIXA-M prepreg tape

Temperature (°C)	260	270	280	300
Viscosity (10^5 Pa.s)	27.9 ± 1	8.26 ± 0.29	2.96 ± 0.4	0.85 ± 0.014

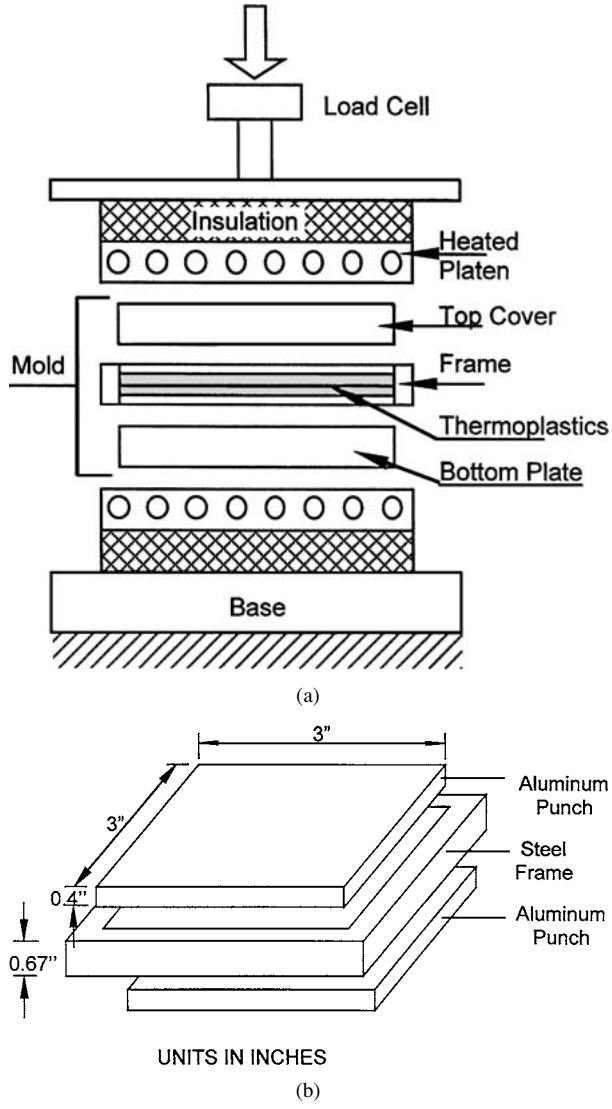

Figure 4 (a) Schematic of the processing setup used in the experimental study and (b) a view of the mold used to prepare the laminate specimens.

A series of experiments were conducted on the fusion bonding of IM-7/PIXA-M prepreg tapes under isothermal conditions for a range of processing pressure, p_{app}, temperature, T, and time, t. The fabrication of IM-7/PIXA-M laminate samples consisted of the following steps: Two $3'' \times 3''$ plies of IM-7/PIXA-M prepreg were placed in an aluminum-steel mold, as shown in Fig. 4b, and subsequently heated in a hot press to a prescribed isothermal temperature. A consolidation pressure was applied until the desired contact time had been attained, and the sample was then removed from the mold to obtain the bonded specimen.

The contact areas at the interface of the bonded samples were analyzed nondestructively using a Matec SR9000 ultrasonic inspection system, with the objective of measuring the degree of intimate contact. The specimens were immersed in a tank filled with water, and examined in the pulse-echo mode. A schematic of the system including its principal components is shown in Fig. 5. A high frequency (30 MHz) focused transducer was used as the source of ultrasonic pulses that insonated the specimens. The reflected waves corresponding to the interlaminar voids were used to detect the non-contacting areas at the interface. The transducer

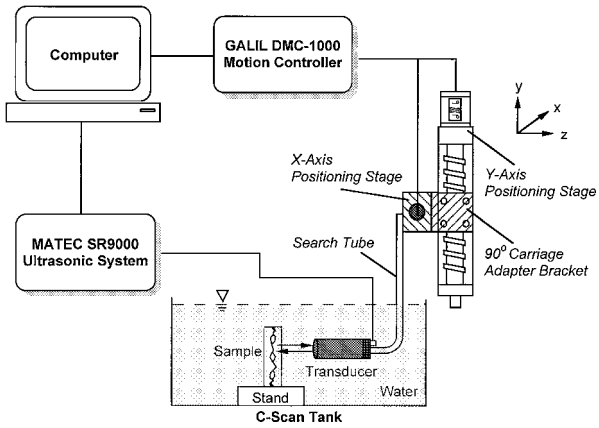

Figure 5 Schematic of the ultrasonic inspection system setup for nondestructive measurement of the degree of intimate contact.

was mounted on a two-axis LINTECH positioning table, which has a spatial accuracy of 0.00025 inches. The axes are driven by two API step motors whose motions are controlled by a GALIL DMC-1000 motion controller. By using the Matec C-Scan software MUIS-32, the transducer is controlled to move in a desired plane parallel to that of the specimen and scan the interface for the contacted and non-contacted areas. Two example C-Scan images are shown in Fig. 6, where black areas indicate interfacial voids. It is visually evident that of the specimens, the one corresponding to Fig. 6b has a higher degree of intimate contact. An analysis of C-Scan images, using any image analysis tool, is used to determine the fraction of the total interface area that is in intimate contact. Referring to Fig. 6, the ratio of the area of the gray regions in the scan to the total area of the specimen denotes the degree of intimate contact. The measured values of the degree of intimate contact were used in the validation of the theoretical model, as discussed in the following section.

5. Results and discussion

The fractal model developed in the preceding sections was implemented numerically to predict the degree of intimate contact as a function of the relevant parameters. A parametric study was conducted to investigate the effects of the various parameters on the intimate contact development, $D_{ic}(t)$, which is influenced by two groups of parameters: manufacturing process related parameters—p_{app}, μ—and the surface geometric parameters, namely, the fractal parameters D, h_0/L_0 and f. For the parametric studies, we focus on the influence of the fractal parameters under specific processing conditions (fixed p_{app} and T). It was found that a maximum of about 10–15 generations in the Cantor set was adequate to describe the intimate contact process because the size of asperities decreases rapidly as n increases and the smaller asperities contribute diminishingly to the intimat contact development.

The results of the parametric studies are presented in Fig. 7, which shows the degree of intimate contact development with time predicted by the fractal model. The influence of the three fractal parameters D, h_0/L_0, and f is studied by fixing two parameters and changing the value of the third. Overall, the degree of intimate contact increases monotonically with time in all the

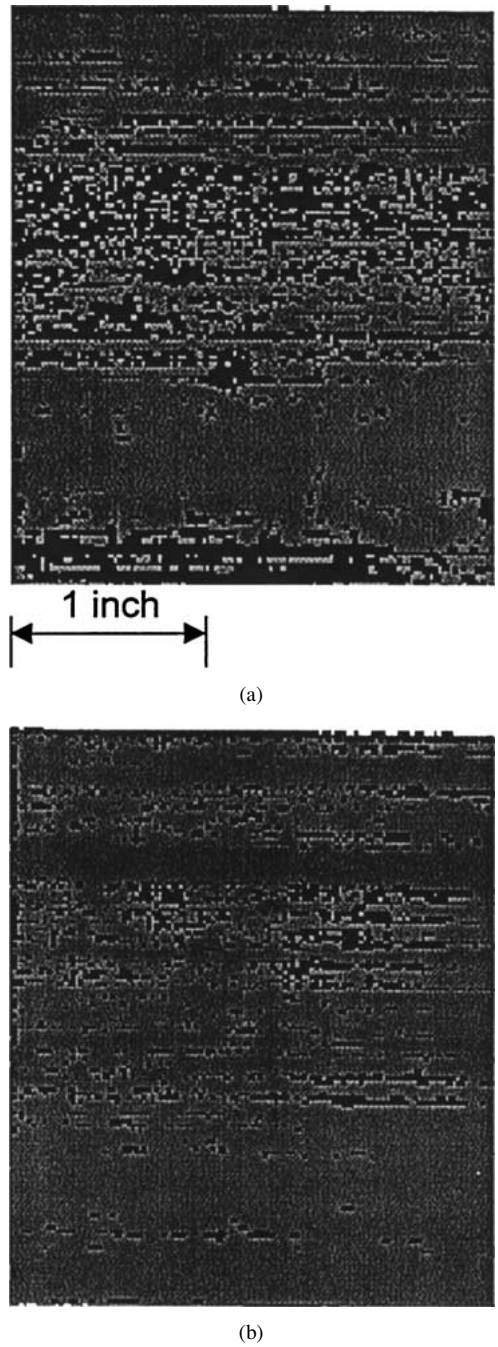

(a)

(b)

Figure 6 Example C-Scan images of the IM-7/PIXA-M test specimen processed under two different conditions. Black areas denote noncontacting areas at the laminate interface.

cases, as physically expected. The effects of the individual parameters are discussed below.

- The fractal dimension, D, determines the degree of "roughness" of a surface. Recall that since D is the fractal dimension of a surface profile, its value lies between 1 and 2. A large magnitude of D within this range means that the profile is more rough and has more apparent asperities—a trend clearly illustrated by Berry and Lewis [11]. Since the effective number of asperities to be flattened increases with increasing roughness, the time needed for intimate contact increases with D as shown in Fig. 7a. Equivalently, the degree of intimate contact achieved in a given amount of time decreases with increasing D.

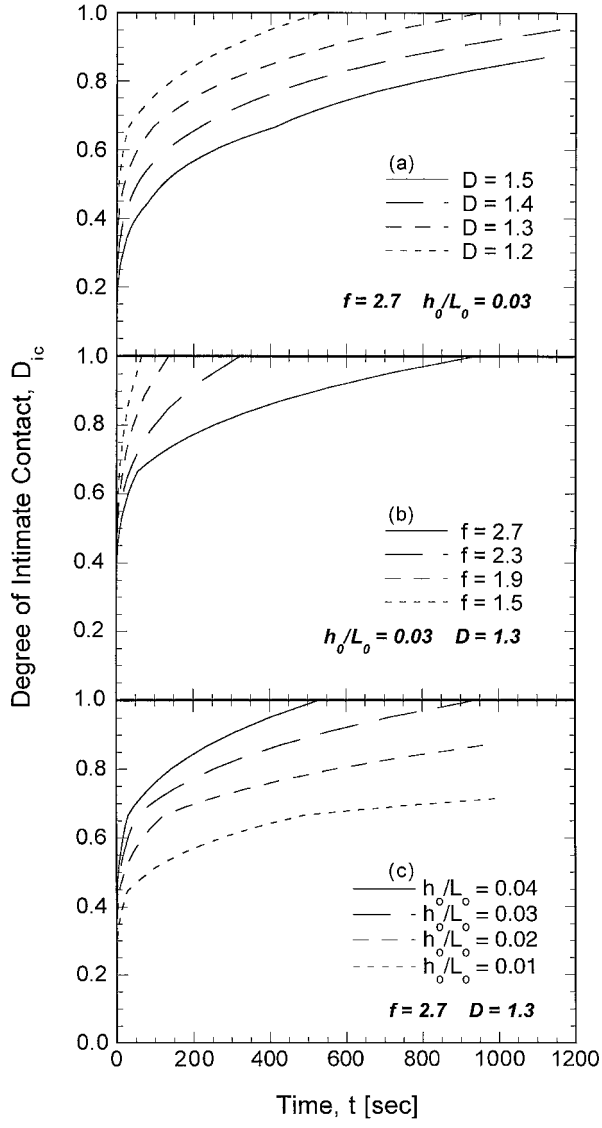

Figure 7 Parametric effects of the fractal surface parameters on the development of degree of intimate contact.

- Fig. 7b illustrates the effect of the parameter f on the intimate contact process. A large magnitude of f corresponds to a greater gap between asperities, which physically corresponds to a larger trough volume to fill up during the process. Hence, a longer time is needed to achieve 100% degree of intimate contact.
- The ratio h_0/L_0 represents the height of the biggest asperity to the profile length. A smaller value of h_0/L_0, therefore, implies that the rough surface is made up of short and wide asperities. As we know, the squeeze flow of a shorter element takes more time, therefore, the time for intimate contact increases as the value of h_0/L_0 decreases. Fig. 7c demonstrates this trend.

In addition to the parametric studies, validation of the model was conducted using experimental data on the intimate contact development during processing of various thermoplastic prepregs. The experimental data were obtained from literature sources [1, 2, 12] as well as from the isothermal processing studies in a hot press described in the previous section. The results of the validation studies are presented in Figs 8–11, as described below.

Fig. 8 shows a comparison of the fractal model with experimental data on the development of the degree of intimate contact with time. The data points were obtained from Dara and Loos [1] and correspond to the consolidation of AS4/polysulfone thermoplastic tapes over a range of processing temperatures and pressures. Since the thermoplastic material was not available for a profilometric scan, the fractal model parameters were determined by a regression fit of the model to the experimental data. The goal of this validation study was therefore primarily that of examining the ability of the model to reflect the physical trends in the data. It is

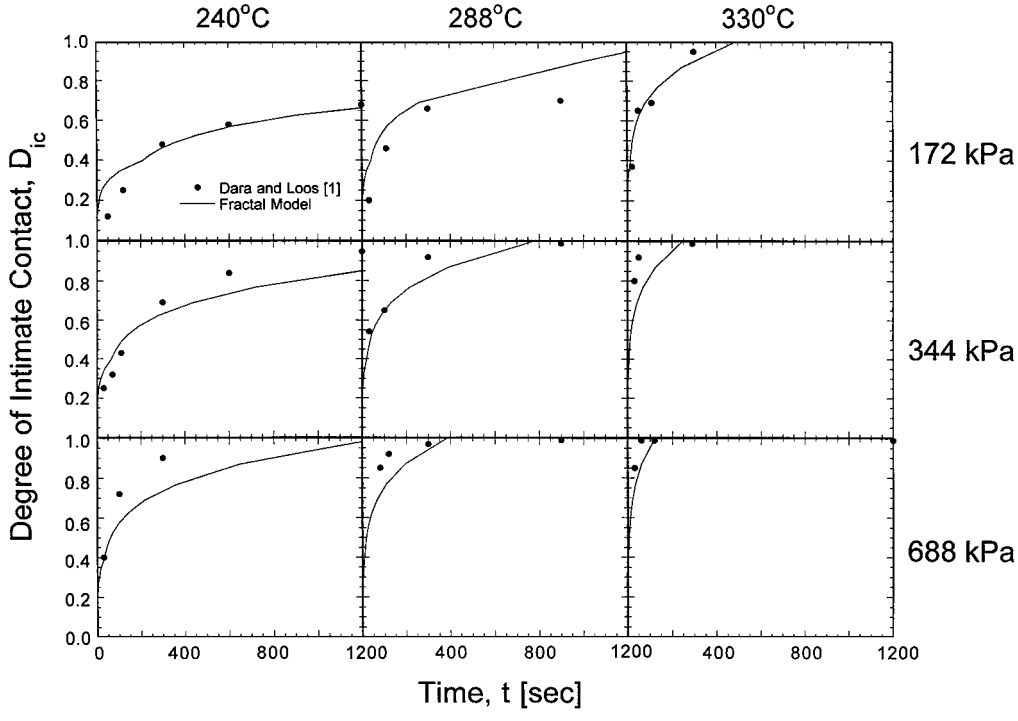

Figure 8 Correlation of the fractal model with experimental data on the processing of AS4/polysulfone tapes.

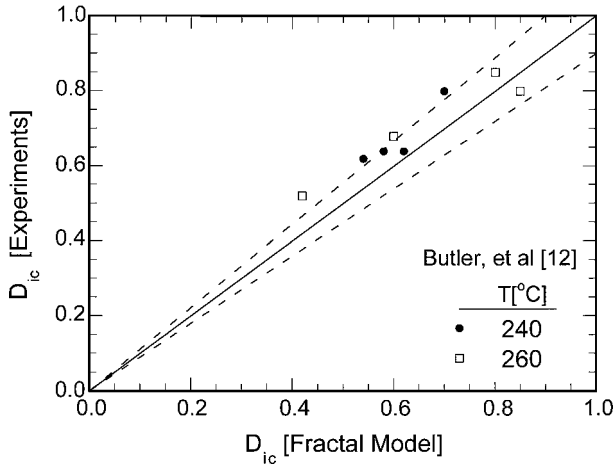

Figure 9 Comparison of the fractal model with experimental data on the processing of AVMID K3A plaques.

evident that the degree of intimate contact increases monotonically with time, and that the time for complete intimate contact decreases with increasing temperature and pressure. The model predictions are seen to accurately follow the trend in the data, and furthermore are in close agreement with the experimentally measured values of the degree of intimate contact.

A general trend observed both in the experimental and the theoretical results in Figs 7 and 8 is that the intimate contact development is initially rapid, but slows down with time. This trend may be explained using the Cantor set model: The smaller, later generation asperities in the Cantor set, which undergo consolidation initially, are spread easily leading to a rapid contact area increase at the beginning of the process. As the process continues, however, the smaller asperities fuse with the larger asperities, which require a longer time for consolidation, thereby slowing down the contact area development.

The model was also verified with experimental data on isothermal bonding of AVMID K3A† plaques [12]. Once again, the thermoplastic surface parameters were determined through a regression fit of the model to experimental data, with the goal of investigating the ability of the model to correlate to experimental measurements. The results are summarized in Fig. 9 where the degree of intimate contact values measured experimentally are plotted with respect to those obtained from the model. The diagonal line in the plot corresponds to the line of exact agreement and the dashed lines denote the 10% error bands. As seen in the figure, the model correlates well with experimental data over the range of parameters considered.

A more direct validation of the model was carried out using the fractal parameters obtained from profilometric measurements on thermoplastic tow surfaces. The studies were conducted on two thermoplastic prepreg materials—AS4/PEEK tows and IM-7/PIXAM tapes. Table I summarizes the values of the measured geometric parameters from the profile scans of the two thermoplastic prepregs. The values of the fractal dimensions point to the significant presence of multiscale

† registered trademark of Dupont Advanced Composites.

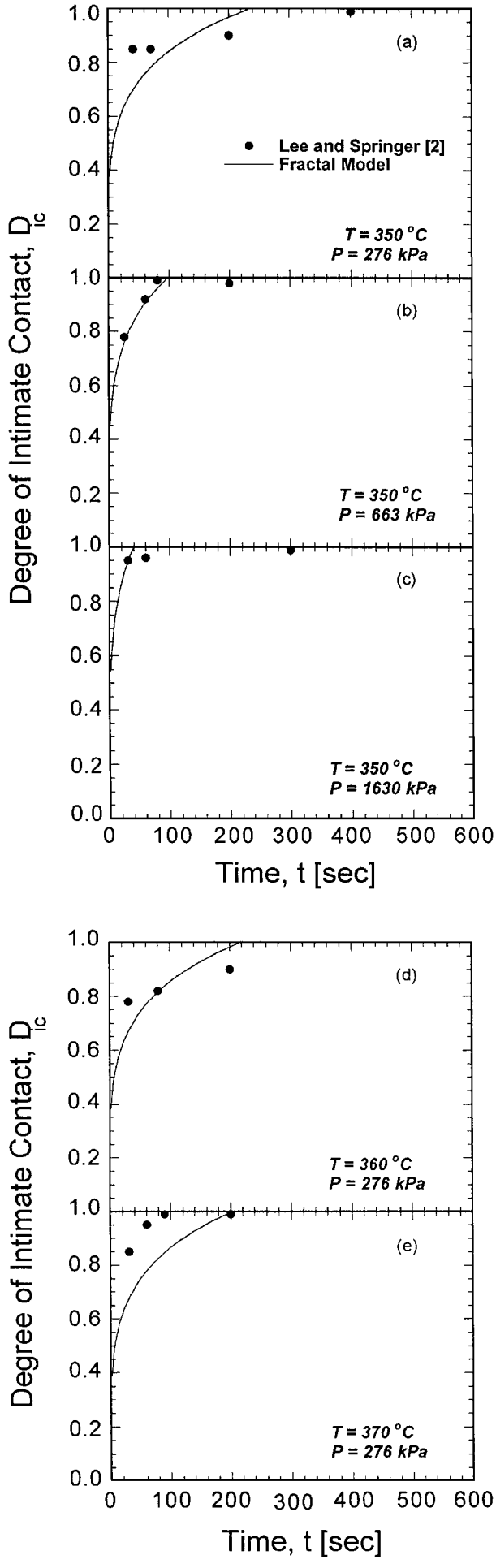

Figure 10 Validation of the fractal model with experimental data on AS4/PEEK prepreg tows.

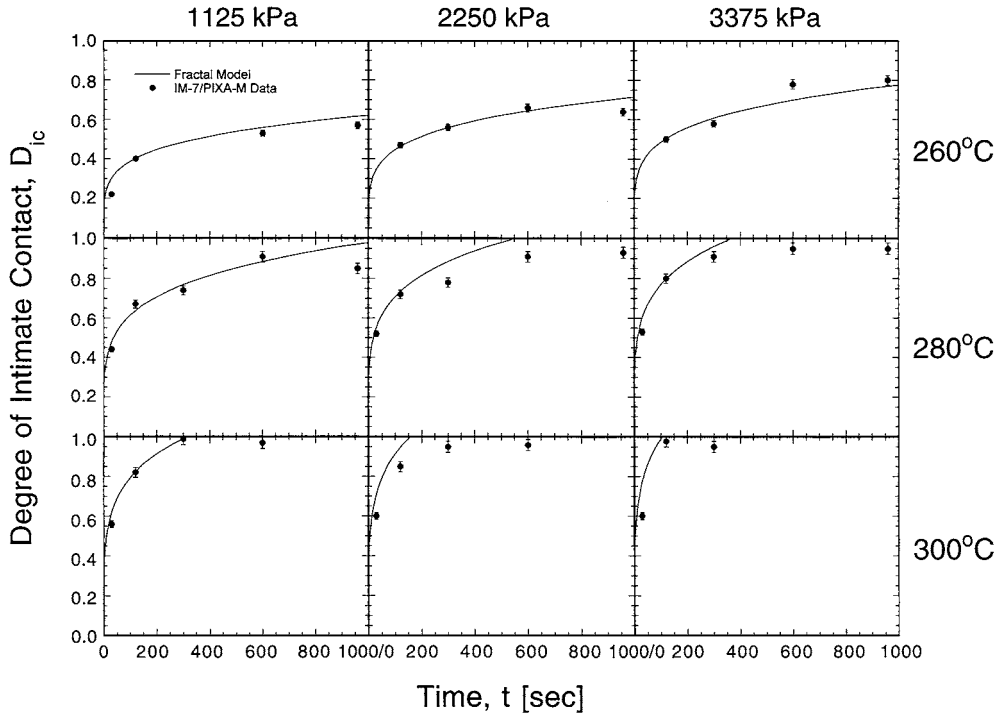

Figure 11 Validation of the fractal model with experimental data on IM-7/PIXA-M prepreg tapes.

features in the asperity structures that can not be ignored. It may be noted from the fractal dimensions, D, and the asperity slenderness parameter values (h_0/L_0) that the IM-7/PIXA-M tape is characterized by relatively rough and shallow asperities in comparison to the AS4/PEEK tows. Physically, therefore, we expect longer times for complete intimate contact in the consolidation of the IM-7/PIXA-M tapes. The measured values of the fractal surface parameters were used in the model to predict the time-dependent intimate contact evolution for the two materials. The model predictions are compared to experimental measurements in Figs 10 and 11, for the AS4/PEEK and IM-7/PIXA-M prepregs, respectively.

Fig. 10 shows the degree of intimate contact development during isothermal consolidation of AS4/PEEK tows over a range of temperatures and pressures. The experimental data in the plots are those reported by Lee and Springer [2], while the model predictions are denoted by the solid lines. The temperature-dependent viscosity of AS4/PEEK given by Mantell and Springer [8] was used in the model predictions. The data comparisons in Fig. 10 reveal a good agreement between the model predictions and the experimental measurements. The intimate contact is seen to evolve rapidly as the pressure is increased, for a fixed temperature (Fig. 10a–c), and as the temperature is increased, for a fixed pressure (Fig. 10a, d, e). Overall, it may be noted that the model tracks the development of interfacial area contact accurately for all the processing conditions shown in Fig. 10.

Further validation of the model was examined for the case of fusion bonding of IM-7/PIXA-M thermoplastic tapes. Since prior experimental data on the processing of these materials is not available in the literature, systematic experiments were conducted as described in the previous section. The processing temperatures ranged from 260°C (which is slightly above the glass transition point of 250°C) to 300°C, and for each temperature, the consolidation pressure was varied from 1.125 MPa to 3.375 MPa. The degree of intimate contact values for the fabricated specimens were evaluated from the ultrasonic C-Scan images of the interface. The prepreg viscosity at the various temperatures, given in Table II, and the surface parameters, listed in Table I, were used in the model to predict the degree of intimate contact as a function of time for the various process parameters. The experimental measurements and the predicted values of the degree of intimate contact are presented in Fig. 11, wherein the solid lines are the model prediction and the symbols denote experimental data along with their respective error bars. Once again, very good agreement is evident between the model predictions and the experimental data over a wide range of the process parameters.

The results presented in this section demonstrate the validity of the fractal model in describing the interlaminar contact evolution during the processing of thermoplastic matrix composites. The fractal description of the geometry gives more realistic representations of thermoplastic prepreg surfaces possessing multiscale characteristics. It was shown that the parameters in the model can be completely measured from roughness measurements, therefore eliminating the need for fitting models to experiments. The generality of the model is evident from the fact that the model could effectively predict and describe all the experimental observations reported in the literature, in addition to those measured as part of the present study, in a unified manner. Since the intimate contact process is a prerequisite for the formation of bond strength, the fractal model in this paper can be coupled with autohesion models [12, 13] to evaluate the interlaminar bond strength in thermoplastic composites, as a function of the process parameters.

6. Conclusions

A fractal model of intimate contact development during thermoplastic fusion bonding was developed based on a Cantor set description of thermoplastic prepreg surfaces. The model parameters, which can be completely determined from surface profile measurements, eliminates the need for "tuning" the models to experimental data. Parametric studies of the surface fractal parameters were presented to illustrate the effects of the geometric parameters on the degree of intimate contact evolution. Experimental validation of the model was presented for diverse thermoplastic materials and processing conditions. A close agreement was demonstrated between the model predictions and experiments. The model developed provides a basis for reliable prediction of interlaminar bonding during thermoplastic composites processing.

Acknowledgements

The work reported in this paper was funded in part by the National Science Foundation (Grant No. CTS-9912093) and the Office of Naval Research (Contract No. N00014-96-1-0726). The AS4/PEEK and IM-7/PIXA-M materials used in the study were provided by Cytec Fiberite, Inc. We gratefully acknowledge their support.

References

1. P. H. DARA and A. C. LOOS, Center for Composite Materials and Structures Report, CCMS-85-10, Virginia Polytechnic Institute and State University, Blacksburg, VA, 1985.
2. W. I. LEE and G. S. SPRINGER, *J. Composite Master*. **21** (1987) 1017.
3. B. B. MANDELBROT, *Phys. Scr*. **32** (1985) 257.
4. A. MAJUMDAR and B. BHUSHAN, *J. Tribology* **112** (1990) 205.
5. F. M. BORODICH and A. B. MOSOLOV, *J. Appl. Math. and Mech*. **56** (1992) 681.
6. T. L. WARREN, A. MAJUMDAR and D. KRAJCINOVIC, *J. Appl. Mech*. **63** (1996) 47.
7. A. MAJUMDAR and B. BHUSHAN, *J. Tribology* **113** (1991) 1.
8. S. C. MANTELL and G. S. SPRINGER, *J. Composite Mater*. **26** (1992) 2348.
9. S. W. CHURCHILL, "Viscous Flows: The Practical Use of Theory" (Butterworths, Boston, 1988) p. 206.
10. C. W. MACOSKO, "Rheology: Principles, Measurements, and Applications" (VCH, New York, 1994) p. 510.
11. M. V. BERRY and Z. V. LEWIS, *Proc. Royal Soc. Lond. A* **370** (1980) 459.
12. C. A. BUTLER, R. L. MCCULLOUGH, R. PITCHUMANI and J. W. GILLESPIE, JR., *J. Thermoplastic Composite Mater*. **11** (1998) 338.
13. R. PITCHUMANI, *et al., Int. J. Heat Mass Transfer* **39** (1996) 1883.

Received 1 September 2000
and accepted 24 April 2001